Article **Journal of Physiotherapy and Medical Technology**
June, 2023 Vol.7 No.17 21-32

Bioinformatic evaluation and *in vivo* study of Orlistat in acute cholestatic damage

Evaluación bioinformática y estudio *in vivo* de Orlistat ante el daño agudo colestásico

ALDABA-MURUATO Liseth Rubí*†, MACÍAS-PÉREZ José Roberto, RODRIGUEZ-RODRIGUEZ Angela and ALVARADO-SÁNCHEZ Brenda

Facultad de Estudios Profesionales Zona Huasteca, Universidad Autónoma de San Luis Potosí. Romualdo del Campo No. 501, Rafael Curiel, C.P. 79060, Ciudad Valles, San Luis Potosí, México

ID 1st Author: *Liseth Rubí, Aldaba-Muruato* / **ORC ID:** 0000-0002-9641-662X, **Researcher ID Thomson:** X-3211-2018, **CVU CONAHCYT ID:** 176507

ID 1st Co-author: *José Roberto, Macías-Pérez* / **ORC ID:** 0000-0001-7925-2494, **Researcher ID Thomson:** X-2998-2018, **CVU CONAHCYT ID:** 172982

ID 2nd Co-author: *Angela, Rodríguez-Rodríguez* / **ORCID ID:** 0009-0009-6706-9954

ID 3rd Co-author: *Brenda*, Alvarado-*Sánchez* / **ORC ID:** 0000-0002-6077-2665, **CVU CONAHCYT ID:** 38716

DOI: 10.35429/JP.2023.17.7.21.32 Received March 10, 2023; Accepted June 30, 2023

Abstract

The incidence of liver diseases increases every year worldwide, making the efforts to prevent them insufficient. The present work evaluated the ability of Orlistat to prevent acute liver injury induced by ligation of the common bile duct (LCBC) in the male Wistar rat. Rats were divided into five experimental groups: untreated (NT), Sham (Sham Surgery), LCBC and LCBC+Orlistat. Serum markers of liver injury as alanine aminotransferase, alkaline phosphatase, gamma-glutamyltranspeptidase, and total and direct bilirubins were significantly increased in LCBC group relative to healthy controls. On the other hand, increases in these markers were significantly prevented in the LCBC+Orlistat group. These results were consistent with observations from livers *in situ* and with H&E-stained histological sections. In addition, the mechanism of action for Orlistat was evaluated through six protein target prediction platforms (ChEMBL, PharmMaper, SEA, Super-PRED, SwissTargetPrediction and TargetNet) where 45 possible molecules with which Orlistat could interact. Our results suggest that Orlistat has hepatoprotective activity during acute damage induced by extrahepatic cholestasis in rats.

Orlistat, Acute liver disease, Common bile duct ligation

Resumen

La incidencia de las enfermedades hepáticas continúa incrementándose cada año en todo el mundo, siendo insuficientes los esfuerzos para prevenirlas. El presente trabajo evaluó la capacidad de Orlistat para prevenir el daño hepático agudo inducido por la ligadura del conducto biliar común (LCBC) en la rata Wistar macho. Las ratas fueron divididas en cinco grupos experimentales: no tratadas (NT), Sham (Cirugía falsa), LCBC y LCBC+Orlistat. Los marcadores séricos de daño hepático alanina aminotransferasa, fosfatasa alcalina, gamma-glutamiltranspeptidasa, y las bilirrubinas totales y directas se incrementaron significativamente en el grupo LCBC en relación con los controles sanos. En el grupo LCBC+Orlistat se previnieron significativamente los aumentos en estos marcadores. Estos resultados fueron consistententes con las observaciones de los hígados in situ y con los cortes histológicos teñidos con H&E. Por otra parte, el mecanismo de acción del Orlistat fue evaluado por medio de seis plataformas de predicción de blancos proteicos (ChEMBL, PharmMaper, SEA, Super-PRED, SwissTargetPrediction y TargetNet) donde se identificaron 45 posibles moléculas con las cuales podría interactuar Orlistat. Nuestros resultados sugieren que el Orlistat posee actividad hepatoprotectora durante el daño agudo inducido por la colestasis extrahepática en rata.

Orlistat, Enfermedad hepática aguda, Ligadura de conducto biliar común

Citation: ALDABA-MURUATO Liseth Rubí, MACÍAS-PÉREZ José Roberto, RODRIGUEZ-RODRIGUEZ Angela and ALVARADO-SÁNCHEZ Brenda. Bioinformatic evaluation and *in vivo* study of Orlistat in acute cholestatic damage. Journal of Physiotherapy and Medical Technology. 2023. 7-17: 21-32

* Correspondence to the Author (e-mail: liseth.aldaba@uaslp.mx)
† Researcher contributing as first author

Introduction

The incidence and complications of liver diseases (HD) continue to increase worldwide (Moon et al., 2020). In Mexico, the HDs with the highest morbidity and mortality rates are cirrhosis and hepatocellular carcinoma (HCC), the latter being the fourth most frequent liver neoplasm in the world (Asrani et al., 2019; Llovet et al., 2021).

The aetiology of HD is multifactorial, the most common being induced by alcohol consumption and the use of drugs or toxicants that are metabolised by the liver (Mohi-Ud-Din, 2019). Obesity and metabolic syndrome favour the development of non-alcoholic steatohepatitis that can culminate in cirrhosis or HCC (Raza et al., 2021). On the other hand, the liver is also susceptible to damage by parasites such as the intestinal protozoan Entamoeba histolytica, which can migrate to the liver and necrotises it, forming an abscess known as an amoebic liver abscess (Ghelfenstein-Ferreira et al., 2020). HD can also be caused by viruses, such as viral hepatitis B and C (Sperry et al., 2022).

Furthermore, it has been reported that regardless of the aetiology, patients with chronic HD such as cirrhosis or HCC who were infected with the SARS-CoV-2 coronavirus type 2, which is the cause of the 2019 coronavirus disease (COVID-19), are vulnerable to serious liver decompensation and dysfunction events (Marjot et al., 2021).

Cholestasis is a liver disorder that occurs due to persistent obstruction of bile flow; this bile retention accumulates toxic components and increases oxidative stress, mainly damaging hepatocytes and cholangiocytes (Salas-Silva et al., 2021). Therefore, intrahepatic cholestasis occurs when alterations of the hepatic parenchyma, bile canaliculi or intrahepatic bile ducts occur, such as in patients with liver cirrhosis, virus-induced hepatitis, inflammation of the biliary tract, and inflammation of the bile ducts (Salas-Silva et al., 2021), inflammation of the bile ducts and HCC, while extrahepatic cholestasis occurs due to involvement of the extrahepatic bile ducts, common hepatic duct, or common bile duct, as in the presence of stones or tumours (Salas-Silva et al. , 2021; Hilscher et al., 2020).

In the present research work, the hepatoprotective capacity of the drug Orlistat ($C_{29}H_{53}NO_5$) was evaluated, which acts by inhibiting pancreatic and gastric lipase, thereby reducing the absorption of lipids from food, and is therefore indicated for the control of obesity (Wong & Cheng-Lai, 2000). In recent years, the scientific community has explored additional biological activities of Orlistat, for example, it was compared to the peptide Ala-Gly-Leu-Gln-Phe-Pro-Val-Gly-Arg (AGL9), a novel hepatoprotective agent, showing similar preventive effects in the non-alcoholic fatty liver disease (NAFLD) model in C57BL/6 mice (Fan et al., 2021).

Likewise, the therapeutic effect of Orlistat was evaluated by its combination with metformin, preventing systemic complications of pancreatitis, gastrointestinal, pulmonary, renal cardiac and nervous system diseases that are induced by COVID-19 in obese diabetic patients (Singh et al., 2021).

Therefore, in the present research work we aimed to determine the ability of Orlistat to reduce cholestatic liver damage that is induced by common bile duct ligation in Wistar rats.

Methodology

Experimental animals

Twenty-nine male Wistar rats (Rattus norvegicus), weighing 200-250 g, were maintained at a constant environmental temperature of 24°C, with light/dark cycles (12 h:12 h). Every day, the rat feeders and drinkers were supplied with rodent food (Labdiet 5008) and drinking water ad libitum.

Ethics

All procedures were performed in accordance with institutional guidelines for the care and use of experimental animals and with the national regulatory standard NOM-062-ZOO-1999. The present research is part of the project entitled "Evaluation of compounds with hepatoprotective activity" accepted by the Research Ethics Committee of the Facultad de Estudios Profesionales Zona Huasteca, UASLP.

ISSN 2523-6849

Experimental protocol

The hepatoprotective capacity of Orlistat was evaluated using the common bile duct ligation (CBDL) model (Van Campenhout et al., 2019; Georgiev et al., 2008). Rats were randomly divided into five groups: NT group: healthy animals without any treatment or surgical procedure (n=3); Sham group: rats were subjected to sham surgery, which consisted of exposing the bile duct without performing ligation, and were further administered prior to Sham surgery, with 1 mL daily for 10 days with 0.25% sodium carboxymethyl cellulose (CMC, Sigma-Aldrich, USA), 0.25% sodium carboxymethyl cellulose (CMC, Sigma-Aldrich, USA), 0.25% sodium carboxymethyl cellulose (CMC, Sigma-Aldrich, USA) and 0.25% sodium carboxymethyl cellulose (CMC, Sigma-Aldrich, USA). (n=4); LCBC group: rats were subjected to a surgical procedure, which allowed identification, isolation, ligation and dissection of the common bile duct, and 10 days prior to surgery, the rats were started daily with 1 mL of CMC 0.25% p.o. and continued to be administered until day 1, and 10 days before surgery, the rats were administered daily with 1 mL of CMC 0.25% p.o., and continued administration until the day of sacrifice (n=9); LCBC+Orlistat group: animals were pre-treated for 10 days with Orlistat 10 mg/kg/day, p.o., prior to LCBC and continued Orlistat administration until the day of sacrifice (n=9); and the Sham+Orlistat group (n=4). All animals were sacrificed 48 h after LCBC or sham surgeries (figure 1).

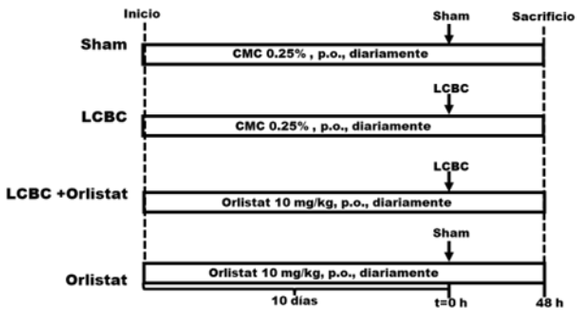

Figure 1 Experimental groups and procedures. Sham: sham surgery; p.o.: from Latin per os (via oral); LCBC: common bile duct ligation. In addition, there was a healthy group that did not undergo any of these procedures (NT group).

Surgical procedure for common bile duct ligation

The rats were anaesthetised with a mixture of Ketamine (80 mg/kg) and Xylazine (10 mg/kg) intraperitoneally (i.p.). The surgeries were performed under sterile conditions, starting with a laparotomy close to the abdominal midline of approximately 1. 5 cm in length, to expose the peritoneal cavity to observe the anatomical position of the liver and access the common bile duct, which was ligated by three knots using sterile non-absorbable surgical suture material (American braided black silk, 4-0 gauge), two knots were made close to the liver and the other at the end of the bile duct close to the duodenum, to finally cut the bile duct before the knot close to the duodenum (Van Campenhout et al., 2019; Georgiev et al., 2008).

Slaughtering the animals

To perform the sacrifices, the rats were anaesthetised with a mixture of Ketamine (80 mg/kg) and Xylazine (10 mg/kg) i.p. Blood was withdrawn by cardiac puncture, which was subsequently centrifuged at 3000 rpm and the serum obtained was used to assess markers of liver damage. The animals were checked for vital signs after blood collection and the liver tissue was dissected. Photographic images of the livers were taken in situ and then carefully dissected and washed in cold physiological saline (NaCl 0.9%) to obtain small fragments that were immersed in 4% neutral formalin and used for histological analysis.

Histological staining

Liver damage was assessed by haematoxylin & eosin (H&E) staining for morphological changes in the tissue and staining with periodic acid and Schiff's reagent (PAS) to determine the presence of carbohydrates in liver cells (Luna, 1968). For these purposes, the liver fragments obtained during animal sacrifice were fixed for 48 h with 4% neutral formalin, then washed with distilled water and subjected to a serial and gradual dehydration process of alcohol baths as follows: 70% ethanol, 85% ethanol, 96% ethanol and 100% ethanol (2 immersions at 60°C for 1 h each). Once the tissues were dehydrated, they were treated by successive baths of absolute ethanol-xylol (50:50) and xylol (2 immersions of 1 h each at 60 °C).

ISSN 2523-6849

Tissues were then embedded in liquid paraffin to create a paraffin block (Ramos-Vara 2017; Sadeghipour & Babaheidarian 2019). From the paraffin block, four micrometre thick liver sections were obtained using a hand-held rotary microtome (ECOSHEL 202A), liver sections were transferred to a flotation bath (~39 °C) and adhered to previously silanised slides (Aragón et al., 2018).

H&E staining

To perform the staining, it is necessary to deparaffinise the tissue at 60 °C for 60 min. Subsequently, the sections were rehydrated by 2 immersions of 40 s in xylene and 1 immersion in absolute ethanol-xylol (50:50), and graded series of 100 % (2 immersions), 96 % and 80 % alcohol and distilled water. Histological sections were stained with Harris haematoxylin (Sigma-Aldrich, USA) for 5 min and rinsed with tap water for 5 min. Immediately, they were immersed in acid alcohol for 10 s and rinsed for 1 min in distilled water and then passed through ammonia water for 35 s and passed through tap water for 1 min. Subsequently, slides were washed for 40 s in 80% ethanol and stained with eosin (Sigma-Aldrich, USA) for 1 min. Finally, tissues were dehydrated with 96%, 100%, alcohol-xyl alcohol (50:50) and xylol (2 dips) for 40 s each (Luna, 1968; Wick, 2019).

PAS staining

Deparaffinised tissues were immersed in 0.5% periodic acid (Sigma-Aldrich, USA) for 5 min, rinsed with distilled water for 20 s, then transferred to Schiff's reagent (Sigma-Aldrich, USA) for 15 min. They were rinsed with tap water for 5 min, then immersed in Mayer's haematoxylin (Sigma-Aldrich, USA) for 10 min and again in tap water for 5 min. Finally, the tissues were dehydrated with 40 s immersions in 96%, 100%, alcohol-xylol (50:50) and xylol (2 immersions) (Luna, 1968).

Microscopic observations

Histological stains were evaluated using an Axiostar plus brightfield microscope (HBO 50/AC, ZESS) with an adapted KOPPACE 16 MP camera (KP-1660), and were processed and analysed with S-Eye (1.6.0.11) and ImageJ (Version: 1.52) software.

Enzyme markers of liver damage in serum

Serum samples were analysed for liver damage by quantifying the enzyme activities of alanine aminotransferase (ALT), alkaline phosphatase (ALP), gamma-glutamyl transferase (GGT) (Reitman & Frankel, 1957; Bergmeyer et al., 1983; Glossmann & Neville, 1972). ALT enzyme activity was assessed in each sample in triplicate, for each test 250 µL of substrate solution (0.2 M D/L-alanine with 2 M α-ketoglutaric acid) and 50 µL of serum were added, mixed and incubated at 37°C for 60 min. Subsequently, 250 µL of the chromogenic reagent (2,4-dinitrophenylhydrazine 1 mM) was added and the sample was incubated again at the same temperature for another 15 min, finally 1.5 mL of 0.4 N NaOH was added.

The reading was done in the spectrophotometer with a wavelength of 515 nm. FA enzyme activity was determined in each sample in triplicate by adding 250 µL of 0.1 M glycine buffer and 1 mM MgCl2 at pH 10.5 and 250 µL of p-nitrophenylphosphate substrate to each sample, mixing and incubating at 37 °C for 5 min, after which time 250 µL of p-nitrophenylphosphate substrate was added to each sample. for 5 min, after which 50 µL of serum was added to incubate again at 37 °C for 30 min, finally 0.02 N NaOH was added and absorbances were measured at a wavelength of 410 nm. In each sample in triplicate, GGT enzyme activities were performed with 400 µL of 0.2 M Tris-HCl reagent, 100 µL of MgCl2, 100 µL of 0. 04 M, 100 µL of 10 mM gamma-glutamyl-p-nitroanilide were added, once the solution was prepared it was incubated for 10 min at 37°C, after this time 200 µL of the serum to be evaluated were added and incubated again for 30 min at the same temperature of 37°C, finally it was removed from incubation and 2 mL of 1.5 M acetic acid was added to stop the reaction, then they were read in a spectrophotometer with a wavelength of 410 nm.

For the three markers of liver damage, blanks were included and the respective standard curves were performed as suggested by the authors.

Total and direct bilirubin in serum

Serum total and direct bilirubin concentrations were also determined following the SPINREACT protocol (Ref: 1001044).

ISSN 2523-6849

Statistical analysis

All results obtained in this work were expressed as means ± standard error (SEM) and statistical analyses were performed using GraphPad Prism 8.00 software by one-way analysis of variance (ANOVA) followed by Tukey's test with $p<0.05$ as the significance level.

Identification of potential protein targets of Orlistat in liver

Six online platforms where protein targets of chemical compounds can be searched or predicted were consulted to analyse what kind of proteins Orlistat might interact with. The platforms used were: ChEMBL (Davies et al., 2015; Méndez et al., 2019), Pharos (Sheils et al., 2021), SEA (Keiser et al., 2007), Super-PRED (Nickel, et al., 2014), SwissTargetPrediction (Daina et al., 2019), and TargetNet (Yao et al., 2016), accessed in August 2023. On these platforms, the Orlistat molecule was entered in mol2 or SMILES formats, generated with OpenBabel software (Cheminfo.org; O'Boyle et al., 2011) where the molecule was plotted for it.

From each set of data obtained in each platform, those with the highest probability of being protein targets were chosen, according to the algorithm used in the platform (Super-PRED, SwissTargetPrediction and TargetNet), or all those returned by the platform were used. For those protein targets chosen, the GeneCards database (GeneCards; Safran et al., 2021) was searched for their homologous protein identification code. With this code, the Human Protein Atlas (Uhlén et al., 2015), a comprehensive compendium that integrates results from omics technologies to map human protein expression in cells, tissues and organs, was consulted.

Results

In situ observations of livers

The in situ livers of the NT, Sham, and Orlistat groups had a normal, dark reddish-brown appearance with shiny, smooth surfaces. The LCBC group presented a light brown liver, which is very different from the livers of the other groups when compared macroscopically. The LCBC+Orlistat group showed an appearance mostly similar to the healthy groups than the LCBC group (figure 2).

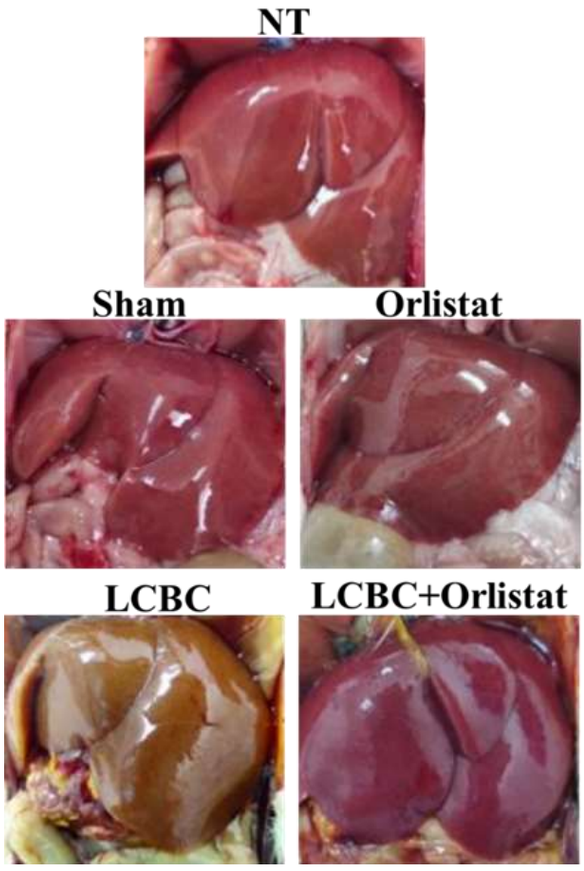

Figure 2 Representative images of livers observed in situ from the different experimental groups

Histological staining

The microscopic observations were consistent with the results in Figure 3, the healthy groups were observed with a well-structured liver parenchyma, while the animals in the LCBC group showed necrosis, inflammation and ductal proliferation, and in the rats of the LCBC+Orlistat group a decrease in liver damage was observed compared to the LCBC group.

ISSN 2523-6849

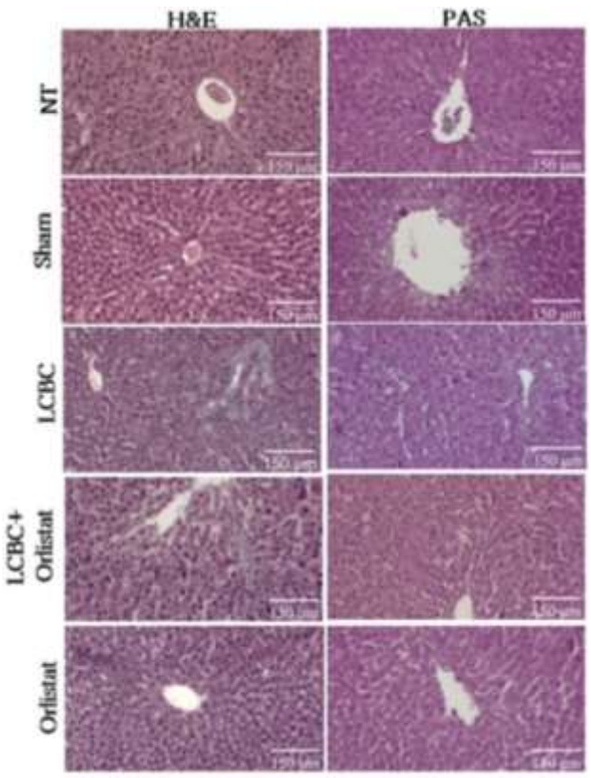

Figure 3 Representative images of histological sections stained with H&E or PAS.

Serum markers of liver damage

ALT, FA and GGT enzyme activities were significantly increased in the LCBC group animals compared to the healthy groups. On the other hand, the LCBC+Orlistat group showed a partial but significant prevention when compared to the healthy and LCBC groups. ALT, FA and GGT enzyme activities were not significantly different between the healthy groups (Figure 4).

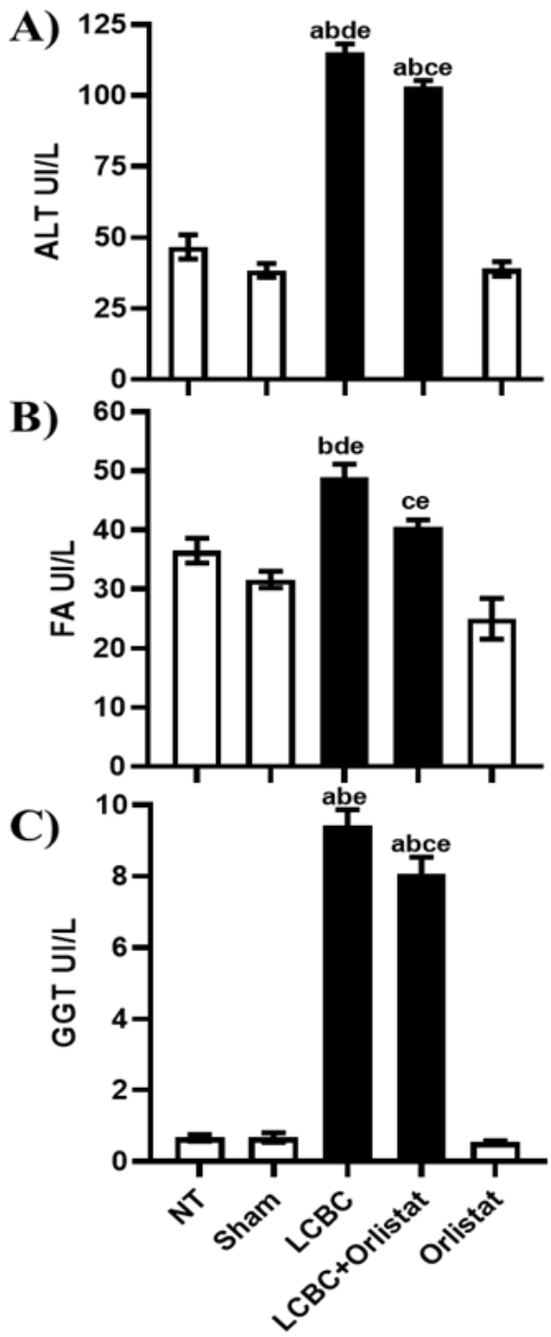

Figure 4 Measurement of liver damage markers in plasma A) ALT, B) FA, C) GGT. Significance $p<0.05$. a: significantly different from NT group; b: significantly different from Sham group; c: significantly different from LCBC group; d: significantly different from LCBC+Orlistat group; e: significantly different from Orlistat group.

Total and direct bilirubin

Total and direct bilirubin increased significantly in the LCBC group, while the LCBC+Orlistat group showed a trend that was not statistically different from the LCBC group. No significant differences were shown between the healthy control groups (Figure 5).

ISSN 2523-6849

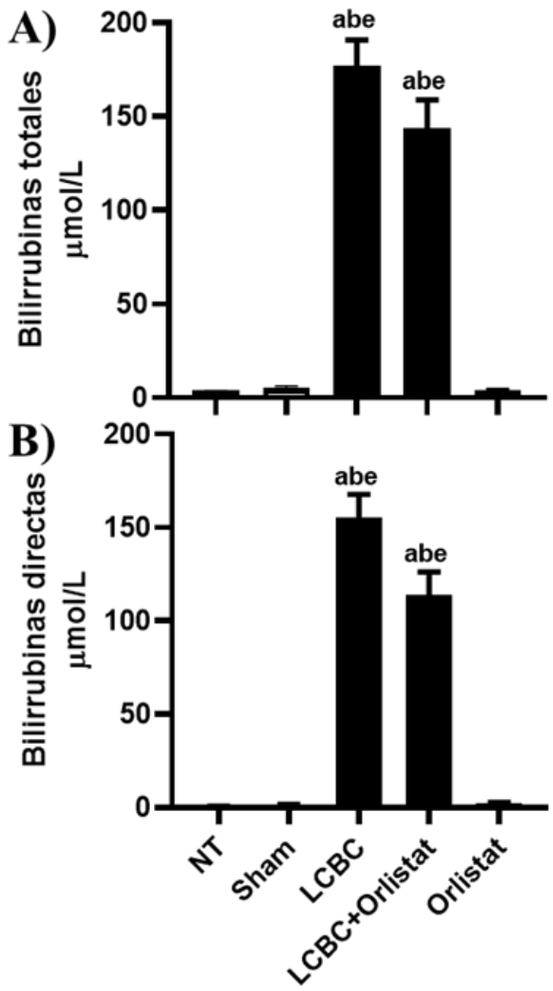

Figure 5 Determination of bilirubin**.** A) Total bilirubin, B) Direct bilirubin. Significance p<0.05. a: significantly different with respect to the NT group; b: different with respect to the Sham group; e: different with respect to the Orlistat group

Identification of potential protein targets of Orlistat in liver

Table 1 shows the 45 potential protein targets of Orlistat that were identified in the different platforms, which were selected based on the information stored in the Human Protein Atlas, either because they are expressed in the liver, enriched in hepatocytes, hepatic stellate cells or Kupffer cells (liver-specific macrophages), as well as for their involvement in liver-specific functions, angiogenesis processes, their relationship with nuclear factor kappa-B (NF□B) or with known prognostic markers of liver cancer. The latter represent 46.6% of Orlistat's potential protein targets. Shown here are the target name, its universal protein identifier code, the selection information from the Human Protein Atlas and the Platform on which it was identified as a potential target.

Tabla 1. Posibles blancos proteicos de Orlistat en hígado.

Nombre de la proteína blanco	ID de la proteína	Ubicación y/o función del blanco	Plataforma de búsqueda de blanco
Bomba de exportación de sales biliares (Bile salt export pump)	ABCB11	Tejido enriquecido: Hígado	Ch
Proteína 1 asociada a la resistencia a múltiples fármacos (Multidrug resistance-associated protein 1)	ABCC1	Marcador pronóstico en cáncer de hígado (no favorable)	SP
Transportador canalicular multiespecífico de aniones orgánicos 1 (Canalicular multispecific organic anion transporter 1)	ABCC2	Tejido, incrementado: Hígado	Ch
Transportador canalicular multiespecífico de aniones orgánicos 2 (Canalicular multispecific organic anion transporter 2)	ABCC3	Tejido, incrementado: Hígado	Ch
Monoacilglicerol lipasa ABHD12 (Monoacylglycerol lipase ABHD12)	ABHD12	Marcador pronóstico en cáncer de hígado (no favorable)	SP, Ch, S, Ph
Monoacilglicerol lipasa ABHD6 (Monoacylglycerol lipase ABHD6)	ABHD6	Tejido, incrementado: Hígado	ST, SP, Ch, S, Ph
ADN-(sitio apurínico o apirimidínico) liasa (DNA-(apurinic or apyrimidinic site) lyase)	APEX1	Marcador pronóstico en cáncer de hígado (no favorable)	SP
Ataxina-2 (Ataxin-2)	ATXN2	Marcador pronóstico en cáncer de hígado (no favorable)	Ch
Homólogo 1 de la proteína Chromobox (Chromobox protein homolog 1)	CBX1	Marcador pronóstico en cáncer de hígado (no favorable)	Ch
Fosfatasa 2 del Inductor de fase M (M-phase inducer phosphatase 2)	CDC25B	Marcador pronóstico en cáncer de hígado (no favorable)	TN
Catepsina B (Cathepsin B)	CTSB	Tipo celular, incrementado: Células de Kupffer	TN
Catepsina L (Cathepsin L)	CTSL	Tipo celular, incrementado: Células estrelladas hepáticas	SP, TN
Citocromo P450 2A6 (Cytochrome P450 2A6)	CYP2A6	Tejido enriquecido: Hígado	SP
Citocromo P450 2C9 (Cytochrome P450 2C9)	CYP2C9	Tejido enriquecido: Hígado	Ch
Citocromo P450 2D6 (Cytochrome P450 2D6)	CYP2D6	Tejido enriquecido: Hígado	Ch
Citocromo P450 3A4 (Cytochrome P450 3A4)	CYP3A4	Tejido enriquecido: Hígado	Ch, SP
Sintasa de ácidos grasos (Fatty acid synthase)	FASN	Angiogénesis (no específica)	Ch, S, Ph
Glutamato carboxipeptidasa 2 (Glutamate carboxypeptidase 2)	FOLH1	Marcador pronóstico en cáncer de hígado (favorable)	TN
Receptor 1 de formil péptido (Formyl peptide receptor 1)	FPR1	Tipo celular enriquecido: Células de Kupffer	SP
Receptor de lipoxina A4 (Lipoxin A4 receptor)	FPR2	Tipo celular, incrementado: Células de Kupffer	SP
Geranilgeranil pirofosfato sintetasa (Geranylgeranyl pyrophosphate synthetase)	GGPS1	Marcador pronóstico en cáncer de hígado (no favorable)	SP
Lipasa hepática (Hepatic lipase)	LIPC	Tejido enriquecido: Hígado	SP, Ch, Ph
Lipasa endotelial (Endothelial lipase)	LIPG	Tipo celular, incrementado: Hepatocitos	SP, Ch, Ph
Acil-proteína tioesterasa 2 (Acyl-protein thioesterase 2)	LYPLA2	Marcador pronóstico en cáncer de hígado (no favorable)	S
Menin (Menin)	MEN1	Marcador pronóstico en cáncer de hígado (no favorable)	Ch*
Monoglicérido lipasa (Monoglyceride lipase)	MGLL	Angiogénesis (no específica)	Ch
Subunidad p105 del factor nuclear NF-kappa-B (Nuclear factor NF-kappa-B p105 subunit)	NFKB1	Subunidad de NFκB	SP
Proteína 1 similar a C1 de Niemann-Pick (Nuclear factor NF-kappa-B p105 subunit)	NPC1L1	Tejido enriquecido: Hígado	Ch
Receptor de pregnano X (Pregnane X receptor)	NR1I2	Tejido enriquecido: Hígado	Ch, SP
PI3-cinasa p110-subunidad delta (PI3-kinase p110-delta subunit)	PIK3CD	Tipo celular, incrementado: Células de Kupffer	SP
PI3-cinasa p110-alfa/p85-alfa (PI3-kinase p110-alpha/p85-alpha)	PIK3R1	Marcador pronóstico en cáncer de hígado (favorable)	SP
Proteína cinasa C delta (Protein kinase C delta)	PRKCD	Marcador pronóstico en cáncer de hígado (no favorable)	SP
Subunidad Macropaín del Proteasoma (Proteasome Macropain subunit)	PSMB2	Marcador pronóstico en cáncer de hígado (no favorable)	Ch
Subunidad Macropaín del Proteasoma, MB1 (Proteasome Macropain subunit MB1)	PSMB5	Marcador pronóstico en cáncer de hígado (no favorable)	Ch
Factor de intercambio de nucleótidos de guanina 3 de Rap (Rap guanine nucleotide exchange factor 3)	RAPGEF3	Angiogénesis (no específica)	Ch
Subunidad beta del factor de unión al núcleo (Core-binding factor subunit beta)	CBFB	Marcador pronóstico en cáncer de hígado (no favorable)	Ch*
Subunidad alfa de la proteína del canal de sodio tipo IV (Sodium channel protein type IV alpha subunit)	SCN4A	Angiogénesis (adipocitos y células endoteliales)	SP
Miembro 1 de la familia 40 de transportadores de solutos (Solute carrier family 40 member 1)	SLC40A1	Tipo celular, incrementado: Células de Kupffer	SP
Miembro 1B1 de la familia de transportadores de aniones orgánicos y transportador de solutos (Solute carrier organic anion transporter family member 1B1)	SLCO1B1	Tejido enriquecido: Hígado	Ch
Miembro 1B3 de la familia de transportadores de aniones orgánicos y transportador de solutos (Solute carrier organic anion transporter family member 1B3)	SLCO1B3	Tejido enriquecido: Hígado	Ch
Tirosil-ADN fosfodiesterasa 1 (Tyrosyl-DNA phosphodiesterase 1)	TDP1	Marcador pronóstico en cáncer de hígado (no favorable)	Ch, SP
Receptor tipo Toll 4 (Toll-like receptor 4)	TLR4	Tipo celular, incrementado: Células de Kupffer, Células estrelladas hepáticas	SP
Proteasa transmembrana serina 6 (Transmembrane protease serine 6)	TMPRSS6	Tejido enriquecido: Hígado	SP
Factor intermediario de transcripción 1-alfa (Transcription intermediary factor 1-alpha)	TRIM24	Marcador pronóstico en cáncer de hígado (no favorable)	SP
Ubiquitina carboxilo-terminal hidrolasa 1 (Ubiquitin carboxyl-terminal hydrolase 1)	USP1	Marcador pronóstico en cáncer de hígado (no favorable)	Ch

El símbolo * indica que el blanco es parte de un complejo proteico, no una proteína individual. Ch-ChEMBL, PM-PharmMapper, Ph-Pharos, S-SEA, SP-Super-PRED, ST-SwissTargetPrediction, TN-TargetNet.

Discussion

Of the liver pathologies, cholestatic diseases are the least studied, so their mechanisms of damage remain poorly understood (Salas-Silva et al., 2021). Cholangiopathies are associated with direct damage to the biliary epithelium and inflammatory processes, such as primary sclerosing cholangitis, primary biliary cholangitis, biliary atresia, cystic fibrosis, drug-induced cholangiopathies, cholangiocarcinoma, among others (Salas-Silva et al., 2019; Guicciardi et al., 2013). In the present study, the hepatoprotective effect of Orlistat on acute liver damage induced by extrahepatic bile duct obstruction was evaluated in Wistar rats. The liver is composed of different cell types, such as hepatocytes, Kupffer cells, hepatic stellate cells, NK (natural killer) cells, hepatic sinusoidal endothelial cells and cholangiocytes, of which hepatocytes and cholangiocytes are the most affected during cholestasis damage (Salas-Silva et al., 2021; Salas-Silva et al., 2019; Guicciardi et al., 2013).

ISSN 2523-6849

In the present work, rats were subjected for a period of 48 h to extrahepatic obstruction of bile flow induced by ligation of the common bile duct, In the LCBC rats, a significant increase in hepatocyte necrosis was observed based on the evaluation of serum ALT enzyme activity and hepatic histological sections stained with H&E and PAS. In addition to evidence of hepatocellular necrosis, increases in cholestasis markers FA and GGT were observed, as well as ductal proliferation, which is another indicator of cholangiocyte damage. Bile ductal proliferation involves massive necrosis of hepatocytes (Guicciardi et al., 2013).

On the other hand, pretreatment with Orlistat in the LCBC+Orlistat group was able to partially prevent liver damage due to cholestasis, observing in situ livers with a macroscopic morphology with fewer alterations compared to the livers of the LCBC group, likewise, histological staining with HE and PAS, Also, histological staining with HE and PAS showed liver parenchymal architecture with less presence of necrosis and bile duct proliferation, and consistent with these observations the liver damage markers ALT, FA and GGT were partially but significantly prevented from increasing in relation to the healthy and LCBC groups. Orlistat is a drug that is prescribed for weight loss, and although in 2010 the FDA (Food and drug administration) announced the existence of clinically attributed liver damage to its use, the hepatotoxicity of Orlistat is considered controversial and far from proven (In LiverTox, 2020).

In the present study, in the group of rats treated only with Orlistat at a dose of 10 mg/kg, p.o., daily (Orlistat group), no enzymatic markers of liver damage were altered, nor were differences in liver architecture observed when compared to the healthy NT and Sham groups. On the other hand, an article was recently published on the effect of Orlistat in the treatment of patients with NAFLD, a disease characterised by excessive lipid accumulation, inflammation and fibrosis, which can progress to cirrhosis or HCC; demonstrating that Orlistat can serve as a treatment in NAFLD (Ye et al., 2019). In addition, Orlistat possesses protective and therapeutic activity in rats with fatty liver disease associated with metabolic dysfunction (MAFLD previously called NAFLD) through activation of nuclear factor erythroid-derived factor 2-like factor 2 (Nrf2), which reduces oxidative stress (Zakaria et al., 2021).

The transcriptional factor Nrf2 is a regulator of the antioxidant response, through antioxidant response element-mediated gene expression, is expressed in many organs, but primarily in liver, enabling liver cells to combat oxidative stress during the development of liver diseases (Tang et al., 2014). However, given the history of its potential hepatotoxicity, further research is needed into its potential uses as a hepatoprotectant and the improvement of dose concentration or combination with other drugs.

Moreover, the present study being one of the first to evaluate the direct effect of Orlistat in a model of in vivo cholestasis liver damage, it was decided to consult online platforms to predict possible molecular targets of Orlistat, which are mainly expressed in the liver, and which could be targets for further research. Of the 45 protein targets identified, the protein coded ABCB11 is a bile salt export pump (BSEP), and mutations in it are associated with cholestatic liver disease (Kubitz et al., 2012), and given the possible interaction with Orlistat, further studies are needed to determine its mechanism of action.

In addition, interest arises in evaluating the bioactive effect of predicted interactions of Orlistat with prognostic markers of liver cancer such as ABCC1, ABHD12, APEX1, ATXN2, CBX1, CDC25B, GGPS1, LYPLA2, MEN1, PRKCD, PSMB2, PSMB5, CBFB, TDP1, TRIM24 and USP1 and identifying possible interaction with (favourable) liver cancer prognostic markers such as CYP2A6, CYP2C9, FOLH1, PIK3R1 and TMPRSS6. Another molecule we identified was NFKB1, which is a suppressor of inflammation and cancer (Cartwright et al., 2016). Orlistat has been shown to reduce colon cancer promotion in mice by suppressing inflammation by inhibiting NFKB activity (Jin et al., 2021).

Therefore, the hepatoprotective results of Orlistat obtained in this work could be mediated by this transcriptional factor, which makes it a molecule that should be explored to try to elucidate the mechanism of action, and a structure activity relationship study (QSAR) would allow the hepatoprotective effect to be optimised.

ISSN 2523-6849

Conclusion

Our results suggest for the first time that Orlistat can reduce cholestatic liver damage induced by acute common bile duct obstruction in Wistar rats. Bioinformatic analysis yields different possible therapeutic targets that open the possibility of diverse mechanisms of action, which can be explored in future projects and the opportunity arises to study the structure-activity relationship with Orlistat analogues and derivatives, in search of optimising its therapeutic effect.

Acknowledgements

The authors are grateful for the technical support of LQC Teresa de Jesús Barrios Hurtado, and also thank CONACYT for the support granted with project 320331, in the framework of the "Basic and/or Frontier Science Modality: Paradigms and Controversies of Science 2022" call for proposals.

Funding

The authors thank CONACYT for funding No. 320331 "Basic and/or Frontier Science Modality: Paradigms and Controversies of Science 2022".

References

Aragón, P., Noguera, P., Bañuls, M. J., Puchades, R., Maquieira, Á., & González-Martínez, M. Á. (2018). Modulating receptor-ligand binding in biorecognition by setting surface wettability. Analytical and bioanalytical chemistry, 410(23), 5723–5730. https://doi.org/10.1007/s00216-018-1247-8

Asrani, S. K., Devarbhavi, H., Eaton, J., & Kamath, P. S. (2019). Burden of liver diseases in the world. Journal of hepatology, 70(1), 151–171. https://doi.org/10.1016/j.jhep.2018.09.014
Bergmeyer, H. U., Grabl, M. & Walter, H. E. (1983). Enzymes, in Methods of Enzymatic Analysis, Edited by J. Bergmeyer, Editor. p. 269 –270.

Cartwright, T., Perkins, N. D., & L Wilson, C. (2016). NFKB1: a suppressor of inflammation, ageing and cancer. The FEBS journal, 283(10), 1812–1822. https://doi.org/10.1111/febs.13627

Cheminfo.org. (2022). OPENBABEL - Chemical file format converter. Cheminfo.org. http://www.cheminfo.org/Chemistry/Cheminformatics/FormatConverter/index.html#

Daina, A., Michielin, O., & Zoete, V. SwissTargetPrediction: updated data and new features for efficient prediction of protein targets of small molecules, 2019, Nucleic Acids Research, 47(W1), W357–W3664. https://doi.org/10.1093/nar/gkz382

Davies, M., Nowotka, M., Papadatos, G., Dedman, N., Gaulton, A., Atkinson, F., Bellis, L., & Overington, J. P. (2015). ChEMBL web services: streamlining access to drug discovery data and utilities. Nucleic acids research, 43(W1), W612–W620. https://doi.org/10.1093/nar/gkv352

Fan, M., Choi, Y. J., Tang, Y., Kim, J. H., Kim, B. G., Lee, B., Bae, S. M., & Kim, E. K. (2021). AGL9: A Novel Hepatoprotective Peptide from the Larvae of Edible Insects Alleviates Obesity-Induced Hepatic Inflammation by Regulating AMPK/Nrf2 Signaling. Foods (Basel, Switzerland), 10(9), 1973. https://doi.org/10.3390/foods10091973

GeneCards - The Human Gene Database. GeneCardsSuite. https://www.genecards.org/

Georgiev, P., Jochum, W., Heinrich, S., Jang, J. H., Nocito, A., Dahm, F., & Clavien, P. A. (2008). Characterization of time-related changes after experimental bile duct ligation. The British journal of surgery, 95(5), 646–656. https://doi.org/10.1002/bjs.6050

Ghelfenstein-Ferreira, T., Gits-Muselli, M., Dellière, S., Denis, B., Guigue, N., Hamane, S., Alanio, A., & Bretagne, S. (2020). Entamoeba histolytica DNA Detection in Serum from Patients with Suspected Amoebic Liver Abscess. Journal of clinical microbiology, 58(10), e01153-20. https://doi.org/10.1128/JCM.01153-20.

Glossmann, H., & Neville, D. M. (1972). gamma-Glutamyltransferase in kidney brush border membranes. FEBS letters, 19(4), 340–344. https://doi.org/10.1016/0014-5793(72)80075-9

ISSN 2523-6849

Guicciardi, M. E., Malhi, H., Mott, J. L., & Gores, G. J. (2013). Apoptosis and necrosis in the liver. Comprehensive Physiology, 3(2), 977–1010. https://doi.org/10.1002/cphy.c120020

Hilscher, M. B., Kamath, P. S., & Eaton, J. E. (2020). Cholestatic Liver Diseases: A Primer for Generalists and Subspecialists. Mayo Clinic proceedings, 95(10), 2263–2279. https://doi.org/10.1016/j.mayocp.2020.01.015

Jin, B. R., Kim, H. J., Sim, S. A., Lee, M., & An, H. J. (2021). Anti-Obesity Drug Orlistat Alleviates Western-Diet-Driven Colitis-Associated Colon Cancer via Inhibition of STAT3 and NF-κB-Mediated Signaling. Cells, 10(8), 2060. https://doi.org/10.3390/cells10082060

Keiser, M. J., Roth, B. L., Armbruster, B. N., Ernsberger, P., Irwin, J. J., & Shoichet, B. K. Relating protein pharmacology by ligand chemistry, 2007, Nature Biotechnology, 25(2), 197–206. https://doi.org/10.1038/nbt1284

Kubitz, R., Dröge, C., Stindt, J., Weissenberger, K., & Häussinger, D. (2012). The bile salt export pump (BSEP) in health and disease. Clinics and research in hepatology and gastroenterology, 36(6), 536–553. https://doi.org/10.1016/j.clinre.2012.06.006

LiverTox: Clinical and Research Information on Drug-Induced Liver Injury [Internet]. Bethesda (MD): National Institute of Diabetes and Digestive and Kidney Diseases; 2012-. Orlistat. [Updated 2020 Jun 4]. Available from: https://www.ncbi.nlm.nih.gov/books/NBK548898/

Llovet, J. M., Kelley. R.K., Villanueva, A., Singal, A. G., Roayaie, S., Lencioni, R., Koike, K., Zucman-Rossi, J., & Finn, R. S. (2021). Hepatocellular carcinoma, Nature reviews Disease Primers, 7, 6. https://doi.org/10.1038/s41572-020-00240-3

Luna, L. G., Manual of histologic staining methods of the Arme Forces Institute of Pathology. 1968. New York: McGraw-Hill. 3rd ed.

Marjot, T., Webb, G. J., Barritt, A. S., 4th, Moon, A. M., Stamataki, Z., Wong, V. W., & Barnes, E. (2021). COVID-19 and liver disease: mechanistic and clinical perspectives. Nature reviews. Gastroenterology & hepatology, 18(5), 348–364. https://doi.org/10.1038/s41575-021-00426-4

Méndez, D., Gaulton, A., Bento, A. P., Chambers, J., De Veij, M., Félix, E., Magariños, M. P., Mosquera, J. F., Mutowo, P., Nowotka, M., Gordillo-Marañón, M., Hunter, F., Junco, L., Mugumbate, G., Rodríguez-López, M., Atkinson, F., Bosc, N., Radoux, C. J., Segura-Cabrera, A., Hersey, A., Leach, A. R. ChEMBL: Towards direct deposition of bioassay data, 2019, Nucleic Acids Research, 47(D1), D930–D940. https://doi.org/10.1093/nar/gky1075

Mohi-Ud-Din, R., Mir, R. H., Sawhney, G., Dar, M. A., & Bhat, Z. A. (2019). Possible Pathways of Hepatotoxicity Caused by Chemical Agents. Current drug metabolism, 20(11), 867–879. https://doi.org/10.2174/1389200220666191105121653

Moon, A. M., Singal, A. G., & Tapper, E. B. (2020). Contemporary Epidemiology of Chronic Liver Disease and Cirrhosis. Clinical gastroenterology and hepatology: the official clinical practice journal of the American Gastroenterological Association, 18(12), 2650–2666. https://doi.org/10.1016/j.cgh.2019.07.060 Nickel, J., Gohlke, B. O., Erehman, J., Banerjee, P., Rong, W. W., Goede, A., Dunkel, M., & Preissner, R. SuperPred: Update on drug classification and target prediction, 2014, Nucleic Acids Research, 42(W1), 26–31. https://doi.org/10.1093/nar/gku477

O'Boyle, N. M., Banck, M., James, C. A., Morley, C., Vandermeersch, T., & Hutchison, G. R. Open Babel: An Open chemical toolbox, 2011, Journal of Cheminformatics 3(10), 33. https://doi.org/10.1186/1758-2946-3-33

Ramos-Vara J. A. (2017). Principles and Methods of Immunohistochemistry. Methods in molecular biology (Clifton, N.J.), 1641, 115–128. https://doi.org/10.1007/978-1-4939-7172-5_5

ISSN 2523-6849

Raza, S., Rajak, S., Upadhyay, A., Tewari, A., & Anthony Sinha, R. (2021). Current treatment paradigms and emerging therapies for NAFLD/NASH. Frontiers in bioscience (Landmark edition), 26(2), 206–237. https://doi.org/10.2741/4892

Reitman, S,. & Frankel, S. (1957). A colorimetric method for the determination of serum glutamic oxalacetic and glutamic pyruvic transaminases. American journal of clinical pathology, 28(1), 56–63. https://doi.org/10.1093/ajcp/28.1.56

Sadeghipour, A., & Babaheidarian, P. (2019). Making Formalin-Fixed, Paraffin Embedded Blocks. Methods in molecular biology (Clifton, N.J.), 1897, 253–268. https://doi.org/10.1007/978-1-4939-8935-5_22

Safran, M., Rosen, N., Twik, M., BarShir, R., Stein, T. I., Dahary, D., Fishilevich, S., & Lancet, D. (2021). The GeneCards Suite. En I. Abugessaisa & T. Kasukawa (Eds.), Practical Guide to Life Science Databases, Springer Singapore, 1a ed., pp. 27–56. https://doi.org/10.1007/978-981-16-5812-9_2

Salas-Silva S, Simoni-Nieves A, López-Ramírez J, Bucio L, Gómez-Quiroz LE, Gutierrez-Ruiz MC, et al. Cholangiocyte death in ductopenic cholestatic cholangiopathies: Mechanistic basis and emerging therapeutic strategies, 2019, Life Sci, 218:324–39.

Salas-Silva, S., Simoni-Nieves, A., Chávez-Rodríguez, L., Gutiérrez-Ruiz, M. C., Bucio, L., & Quiroz, L. E. G. (2021). Mechanism of cholangiocellular damage and repair during cholestasis. Annals of hepatology, 26, 100530. https://doi.org/10.1016/j.aohep.2021.100530

Sheils, T. K., Mathias, S. L., Kelleher, K. J., Siramshetty, V. B., Nguyen, D. T., Bologa, C. G., Jensen, L. J., Vidović, D., Koleti, A., Schürer, S. C., Waller, A., Yang, J. J., Holmes, J., Bocci, G., Southall, N., Dharkar, P., Mathé, E., Simeonov, A., & Oprea, T. I. TCRD and Pharos 2021: Mining the human proteome for disease biology, 2021. Nucleic Acids Research, 49(D1), D1334–D1346. https://doi.org/10.1093/nar/gkaa993

Singh, Y., Gupta, G., Anand, K., Kumar Jha, N., Thangavelu, L., Kumar Chellappan, D., & Dua, K. (2021). Molecular exploration of combinational therapy of orlistat with metformin prevents the COVID-19 consequences in obese diabetic patients. European review for medical and pharmacological sciences, 25(2), 580–582. https://doi.org/10.26355/eurrev_202101_24614

Sperry, A. B., Bennett, A., & Wen, J. (2022). Hepatitis B and C in Children. Clinics in liver disease, 26(3), 403–420. https://doi.org/10.1016/j.cld.2022.03.005

Tang, W., Jiang, Y. F., Ponnusamy, M., & Diallo, M. (2014). Role of Nrf2 in chronic liver disease. World journal of gastroenterology, 20(36), 13079–13087. https://doi.org/10.3748/wjg.v20.i36.13079

Uhlén, M., Fagerberg, L., Hallström, B. M., Lindskog, C., Oksvold, P., Mardinoglu, A., Sivertsson, Å., Kampf, C., Sjöstedt, E., Asplund, A., Olsson, I., Edlund, K., Lundberg, E., Navani, S., Szigyarto, C. A.-K., Odeberg, J., Djureinovic, D., Takanen, J. O., Hober, S., … Pontén, F. Tissue-based map of the human proteome. Science, 2015, Proteomics. New York, N.Y., 347(6220), 1260419. https://doi.org/10.1126/science.1260419

Van Campenhout, S., Van Vlierberghe, H., & Devisscher, L. (2019). Common Bile Duct Ligation as Model for Secondary Biliary Cirrhosis. Methods in molecular biology (Clifton, N.J.), 1981, 237–247. https://doi.org/10.1007/978-1-4939-9420-5_15

Wick M. R. (2019). The hematoxylin and eosin stain in anatomic pathology-An often-neglected focus of quality assurance in the laboratory. Seminars in diagnostic pathology, 36(5), 303–311. https://doi.org/10.1053/j.semdp.2019.06.003

Wong, N. N., & Cheng-Lai, A. (2000). Orlistat. Heart disease (Hagerstown, Md.), 2(2), 174–181.

Yao, Z. J., Dong, J., Che, Y. J., Zhu, M. F., Wen, M., Wang, N. N., Wang, S., Lu, A. P., & Cao, D. S. TargetNet: a web service for predicting potential drug–target interaction profiling via multi-target SAR models, 2016, Journal of Computer-Aided Molecular Design, 30(5), 413–424. https://doi.org/10.1007/s10822-016-9915-2

ISSN 2523-6849

Ye, J., Wu, Y., Li, F., Wu, T., Shao, C., Lin, Y., Wang, W., Feng, S., & Zhong, B. Effect of orlistat on liver fat content in patients with nonalcoholic fatty liver disease with obesity: assessment using magnetic resonance imaging-derived proton density fat fraction, 2019, Therapeutic advances in gastroenterology, 12, 1756284819879047. https://doi.org/10.1177/1756284819879047

Zakaria, Z., Othman, Z. A., Bagi Suleiman, J., Jalil, N. A. C., Ghazali, W. S. W., & Mohamed, M. (2021). Protective and Therapeutic Effects of Orlistat on Metabolic Syndrome and Oxidative Stress in High-Fat Diet-Induced Metabolic Dysfunction-Associated Fatty Liver Disease (MAFLD) in Rats: Role on Nrf2 Activation. Veterinary sciences, 8(11), 274. https://doi.org/10.3390/vetsci8110274

ISSN 2523-6849